Chemical Science

ROYAL SOCIETY OF CHEMISTRY

EDGE ARTICLE

View Article Online
View Journal | View Issue

Cite this: *Chem. Sci.*, 2023, **14**, 14302

All publication charges for this article have been paid for by the Royal Society of Chemistry

Received 30th October 2023
Accepted 24th November 2023

DOI: 10.1039/d3sc05770d

rsc.li/chemical-science

$(C_5H_{6.16}N_2Cl_{0.84})(IO_2Cl_2)$: a birefringent crystal featuring unprecedented $(IO_2Cl_2)^-$ anions and π-conjugated organic cations†

Qian-Qian Chen,[ab] Chun-Li Hu,[a] Ming-Zhi Zhang[ab] and Jiang-Gao Mao *[ab]

Birefringent crystals can manipulate the polarization state of lasers and have vital application in polarizers, optical isolators, phase compensators, *etc.* The design and synthesis of crystals with large birefringence remains a challenging task. To design crystals with large birefringence, we combine an unprecedented chloroiodate(v) group $(IO_2Cl_2)^-$ featuring large polarizability anisotropy and a strong stereochemically active lone pair (SCALP) with the π-conjugated 2-amino-5-chloropyridine group. The superior synergy effect of $(IO_2Cl_2)^-$ and 2-amino-5-chloropyridine groups produces a new birefringent crystal, namely $(C_5H_{6.16}N_2Cl_{0.84})(IO_2Cl_2)$. It exhibits remarkably large birefringence of 0.67 at 546 nm, far exceeding those of most visible birefringent materials reported. This work discovers the first chloroiodate(v) group and provides a new synthetic route for birefringent materials.

Introduction

Birefringent crystals could modulate the polarization-dependent light propagation, and they are widely applied in optical isolators, polarizers, and phase compensators.[1–6] The crystals with giant optical anisotropy could effectively manipulate light and miniaturize the fabricated devices.[6] In the visible region, the materials show relatively small birefringence (below 0.3) such as commercialized YVO_4 ($\Delta n_{exp.}$: 0.204 at 532 nm) and $CaCO_3$ ($\Delta n_{exp.}$: 0.172 at 589 nm).[7,8] Only a few crystals exhibit birefringence greater than 0.5, such as $Cd(H_2C_6N_7O_3)_2\cdot 8H_2O$ ($\Delta n_{exp.}$: 0.60 at 550 nm) and $SnPO_4I$ ($\Delta n_{exp.}$: 0.664 at 546 nm).[9–11] However, $Cd(H_2C_6N_7O_3)_2\cdot 8H_2O$ suffers from low thermal stability (85 °C), and $SnPO_4I$ (band gap: 2.45 eV) shows a limited visible transparency window. The birefringence of $Cd(H_2C_6N_7O_3)_2\cdot 8H_2O$ and $SnPO_4I$ arises from the π-conjugated $(H_2C_6N_7O_3)^-$ groups and SCALP Sn(II)-based groups, respectively. Numerous studies illustrate that π-conjugated groups and SCALP groups are efficient birefringent-active groups, and incorporating these groups regularly can result in large birefringence.[4,10–14]

Besides the Sn(II)-based materials, metal iodates containing strong SCALPs are also a class of promising visible birefringent crystals.[15,16] The birefringence of most iodates is in the range of 0.05–0.25 as exemplified by $CsIO_3$ ($\Delta n_{cal.}$: 0.19 at 1064 nm).[17–20] Partial substitution of oxygen atoms with fluorine atoms afforded fluoroiodate groups such as $(IO_3F)^{2-}$ and $(IO_2F_2)^-$, which show larger polarizability anisotropy than IO_3^- groups.[21] About 83% of the reported fluoroiodates are assembled from $(IO_2F_2)^-$ groups but show relatively small birefringence (Δn: 0.05–0.20) as exemplified by $CsIO_2F_2$ ($\Delta n_{cal.}$: 0.046 at 1064 nm).[19–22] The large electronegativity of F causes the F-2p states to locate at a low energy, usually playing a negative role in birefringence.[22–24] To get out of the dilemma, we select the Cl atom with lower electronegativity to design the chloroiodate(v) group $(IO_2Cl_2)^-$. According to our calculations, the large difference in I–Cl and I–O bond lengths of $(IO_2Cl_2)^-$ groups generates polarizability anisotropy which is about five times larger than that of $(IO_3)^-$ and $(IO_2F_2)^-$ groups. The strength of SCALPs on $(IO_2Cl_2)^-$ groups would be enhanced due to the strong interaction of I-5s5p and Cl-3p states near the Fermi level, favouring large birefringence.[11–14] However, no chloroiodate(v) has been reported so far, probably due to the difficulty of replacing strong I–O bonds with weak I–Cl bonds. The $(IO_2Cl_2)^-$ was only reported theoretically as a transient intermediate, reflecting its possible existence.[25]

π-conjugated groups possessing delocalized p_π electrons and prominent polarizability anisotropy can also serve as perfect birefringent-active groups, such as NO_3^-, $(B_3O_6)^{3-}$, $(H_2C_6N_7O_3)^-$, $(H_xC_3N_3O_3)^{(3-x)-}$, $(H_xC_6N_9)^{(3-x)-}$ (x = 0, 1, 2), $[C(NH_2)_3]^+$ and $(C_5H_6NO)^+$.[10,15,26–33] The introduction of π-conjugated groups into metal iodates can enhance birefringence significantly, as exemplified by $Sc(IO_3)_2(NO_3)$ ($\Delta n_{exp.}$: 0.348 at 546 nm).[15,28,33] Herein we select the π-conjugated 2-amino-5-chloropyridine group featuring a push–pull electronic

[a]*State Key Laboratory of Structural Chemistry, Fujian Institute of Research on the Structure of Matter, Chinese Academy of Sciences, Fuzhou, 350002, P. R. China. E-mail: mjg@fjirsm.ac.cn*

[b]*University of Chinese Academy of Sciences, Beijing 100039, P. R. China*

† Electronic supplementary information (ESI) available: Experimental procedures, theoretical calculations, crystallographic data, and measurements of physical properties. CCDC 2300002. For ESI and crystallographic data in CIF or other electronic format see DOI: https://doi.org/10.1039/d3sc05770d

structure and intramolecular charge transfer, which can promote p_π electron delocalization and polarizability anisotropy.[34] The combination of SCALP chloroiodate(v) groups and π-conjugated 2-amino-5-chloropyridine groups led to a new birefringent crystal, namely, $(C_5H_{6.16}N_2Cl_{0.84})(IO_2Cl_2)$. It shows enormous birefringence ($\Delta n_{exp.}$: 0.67 at 546 nm), exceeding those of most visible birefringent materials reported.

Results and discussion

Crystals of $(C_5H_{6.16}N_2Cl_{0.84})(IO_2Cl_2)$ were successfully grown by the evaporation method in aqueous hydrochloric acid media (see ESI†). The $(IO_2Cl_2)^-$ group is formed at a high HCl/HIO_3 molar ratio of 3 : 1 due to the much stronger I–O bonds compared with I–Cl bonds. Under such conditions, one H atom on the meta position of 2-aminopyridine is partially replaced by the Cl(3) atom with a Cl/H ratio of 0.84 : 0.16, leading to the formation of the $(C_5H_{6.16}N_2Cl_{0.84})^+$ cation, which is similar to the conversion of 2-aminopyridine to 2-amino-5-chloropyridine (see ESI†).[35]

The crystals of $(C_5H_{6.16}N_2Cl_{0.84})(IO_2Cl_2)$ are shown in Fig. S1.† Its purity was confirmed by powder X-ray diffraction (Fig. S2, ESI†). The results of elemental analysis are close to the calculated values (see ESI†). The existence of I and Cl was confirmed by energy-dispersive X-ray spectroscopy (Fig. S3 and S4, ESI†). $(C_5H_{6.16}N_2Cl_{0.84})(IO_2Cl_2)$ crystallizes in the triclinic space group *P*-1 (no. 2) (Tables S1–S4, ESI†). Its asymmetric unit consists of one $(C_5H_{6.16}N_2Cl_{0.84})^+$ cation and one $(IO_2Cl_2)^-$ anion, and all of the atoms are located at the general sites. In the $(C_5H_{6.16}N_2Cl_{0.84})^+$ cation, the bond lengths of C–C, C–N, and C–Cl are in the ranges of 1.344(5)–1.410(5) Å, 1.325(4)–1.360(4) Å, and 1.715(4) Å, respectively. The I(1) atom is four-coordinated by two O atoms and two Cl atoms to form a seesaw-shaped $(IO_2Cl_2)^-$. The two I–Cl bond lengths (2.4929(8) and 2.4963(8) Å) are much longer than the two I–O bond lengths (1.784(2) and 1.791(2) Å), and the Cl–I–Cl and O–I–O bond angles are 172.75(3)° and 99.6(1)°, respectively. These I–O and I–Cl bond lengths are close to those of IO_3^- groups (1.73(3)–1.89(2) Å) and $(ICl_4)^-$ groups (2.497(1)–2.515(1) Å) reported previously.[17–20,36] The calculated bond valence value of I(1) is 5.048, confirming its oxidation state of +5.[37]

In $(C_5H_{6.16}N_2Cl_{0.84})(IO_2Cl_2)$, two $(C_5H_{6.16}N_2Cl_{0.84})^+$ cations and two $(IO_2Cl_2)^-$ anions are interconnected through hydrogen bonds (N(1)–H(1)···O(2) 2.875(3) Å, N(2)–H(2A)···O(2) 2.999(4) Å and N(2)–H(2B)···O(1) 2.994(4) Å) into a $[(C_5H_{6.16}N_2Cl_{0.84})(IO_2Cl_2)]_2$ dimeric unit (Fig. 1a). These dimeric units are interlinked into a three-dimensional (3D) supramolecular structure through π–π stacking interactions with an inter-ring distance of 3.75 Å between neighboring parallel $(C_5H_{6.16}N_2Cl_{0.84})^+$ cations (Fig. 1b).

Thermogravimetric analysis demonstrated that $(C_5H_{6.16}N_2Cl_{0.84})(IO_2Cl_2)$ is thermally stable up to 110 °C, after which it is totally decomposed in one step from 110 °C to 1000 °C (Fig. S5, ESI.† The infrared (IR) spectrum is shown in Fig. S6† and the detailed assignments of the IR bands are presented in Table S5.† (ref. 38) The peaks located at 890–650 cm^{-1} signify the I–Cl and I–O stretching vibrations, and the absorption bands

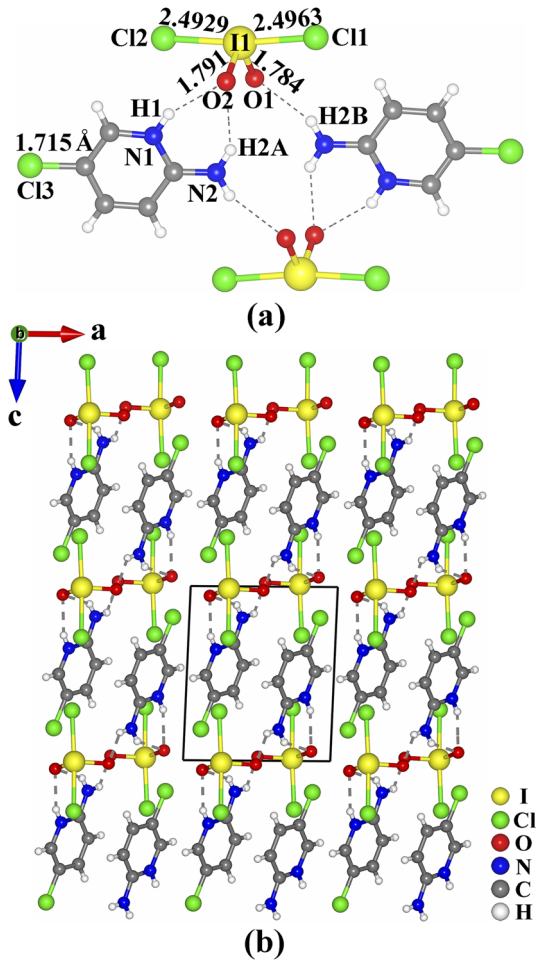

Fig. 1 Views of the $[(C_5H_{6.16}N_2Cl_{0.84})(IO_2Cl_2)]_2$ dimeric unit (a), and the structure of $(C_5H_{6.16}N_2Cl_{0.84})(IO_2Cl_2)$ (b).

observed at 650–400 cm^{-1} correspond to the I–Cl and I–O bending vibrations. The UV-vis-NIR diffuse reflectance spectrum revealed its UV absorption cutoff edge of 325 nm, and its band gap of 3.38 eV (Fig. S7, ESI†). The band gap is larger than those of some outstanding birefringent materials such as Sn_2PO_4I (2.45 eV) and $(C_3N_6H_8)PbBr_4$ (3.13 eV), but is smaller than those of some pyridine iodates, fluoroiodates and iodate chlorides such as $[o\text{-}C_5H_4NHOH]_2[I_7O_{18}(OH)]\cdot 3H_2O$ (3.90 eV), $CsIO_2F_2$ (4.5 eV) and $Ba(IO_3)Cl$ (4.32 eV).[11,20,28,39,40] Under the excitation at 365 nm, $(C_5H_{6.16}N_2Cl_{0.84})(IO_2Cl_2)$ displays a blue emission band maximizing at 410 nm (Fig. S8, ESI†), but its photoluminescence quantum yield is less than 1%. A significant blue shift relative to the neutral 2-amino-5-chloropyridine is observed probably due to the protonation of the organic molecule and the effect of $(IO_2Cl_2)^-$ on its HOMO and LUMO.[41]

Based on the polarizing microscope method, the birefringence of $(C_5H_{6.16}N_2Cl_{0.84})(IO_2Cl_2)$ was measured at $\lambda = 546$ nm using the (010) crystal plane (Fig. 2 and S9, S10†). The optical path difference is 15172.51 nm, and the thickness of the measured crystal is 22.7 μm. The experimental birefringence of $(C_5H_{6.16}N_2Cl_{0.84})(IO_2Cl_2)$ is 0.67 at 546 nm. Its birefringence obviously exceeds those of most visible birefringent materials

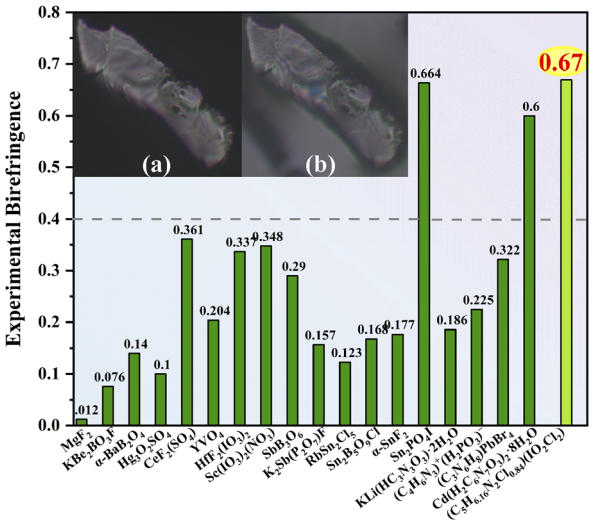

Fig. 2 Comparison of birefringence of some excellent birefringent materials at 514–550 nm. The embedded graphs: the original crystal of $(C_5H_{6.16}N_2Cl_{0.84})(IO_2Cl_2)$ under the cross-polarized light (a), and the crystal achieving complete extinction (b).

reported, such as $CsIO_3$ ($\Delta n_{cal.}$: 0.19 at 1064 nm), $RbIO_2F_2$ ($\Delta n_{cal.}$: 0.058 at 1064 nm), $SrI_2O_5F_2$ ($\Delta n_{cal.}$: 0.203 at 532 nm), $Ba(IO_3)Cl$ ($\Delta n_{cal.}$: 0.118 at 1064 nm), $Rb_2HC_3N_3O_3$ ($\Delta n_{cal.}$: 0.4 at 532 nm), $Cd(H_2C_6N_7O_3)_2\cdot 8H_2O$ ($\Delta n_{exp.}$: 0.60 at 550 nm), and $Sc(IO_3)_2(NO_3)$ ($\Delta n_{exp.}$: 0.348 at 546 nm).[8,10–22,30–32,39,40,42–51]

Band-structure calculations *via* the density functional theory indicated that $(C_5H_{6.16}N_2Cl_{0.84})(IO_2Cl_2)$ has a direct band gap of 2.94 eV, which is smaller than the experimental band gap of 3.38 eV (Fig. S11, ESI†). The scissor operator of 0.44 eV was applied for calculating birefringence. In the partial density of states (PDOS) diagram (Fig. S12, ESI†), the topmost valence band (VB) and the bottommost conduction band (CB) are mainly comprised of C-2p and N-2p states. Hence, the band gap of $(C_5H_{6.16}N_2Cl_{0.84})(IO_2Cl_2)$ is dominated by $(C_5H_{6.16}N_2Cl_{0.84})^+$. In the PDOS, the strong interaction of I-5s5p and Cl-3p states near the Fermi level is beneficial for the strength of SCALPs on I^{5+}, which is positively related to the birefringence.[11–14] The SCALP of the $(IO_2Cl_2)^-$ group could be visually comprehended from an electron density difference (EDD) map (Fig. 3a). The seesaw-shaped $(IO_2Cl_2)^-$ group could be also seen as a trigonal bipyramid with one of the trigonal vertexes occupied by the SCALP.

Under $\lambda = 546$ nm, the calculated refractive index features $n_z \gg n_y > n_x$ along the principal dielectric axes (Fig. S13, ESI†). The angles between the crystallographic axes and the principal dielectric axes are shown in Table S6 (ESI†). The calculated birefringence of $(C_5H_{6.16}N_2Cl_{0.84})(IO_2Cl_2)$ is 0.67 at 546 nm, which matches with the experimental result.

The mechanism of birefringence is analysed below. First, the $(C_5H_{6.16}N_2Cl_{0.84})^+$ and $(IO_2Cl_2)^-$ groups display large polarizability anisotropies of 71.1 and 69.3, respectively, which are approximately five times greater than those of IO_3^- and $IO_2F_2^-$ groups (Fig. 3b). Second, the $(C_5H_{6.16}N_2Cl_{0.84})^+$ groups are aligned perfectly in parallel and deviate from the (100) crystal plane with a dihedral angle of 43.8°. Thus, $\Delta n = n_{in\text{-}plane} - n_{out\text{-}plane} = n(100) - n_x$.[10] Third, from the EDD map (Fig. S14, ESI†), the SCALPs manifest regular arrangements in the direction deviating from the *y*-axis by 18.9°, and the polarizable I–Cl bonds deviate from the *z*-axis by 5.6°, which leads to $n_z \gg n_y$.[13,52] So, $\Delta n = n(100) - n_x = n_z - n_x = n(010)$. The $(IO_2Cl_2)^-$ and $(C_5H_{6.16}N_2Cl_{0.84})^+$ groups are both located in suitable locations and fastened by hydrogen bonds, which prominently enhances the (010) in-plane anisotropy and thus leads to the large birefringence.[52]

To intuitively unveil the source of birefringence of $(C_5H_{6.16}N_2Cl_{0.84})(IO_2Cl_2)$, polarizability anisotropy-weighted electron density (PAWED) is displayed in Fig. 3c and d. In the VB, the nonbonding Cl-3p and O-2p of $(IO_2Cl_2)^-$, and the p states in

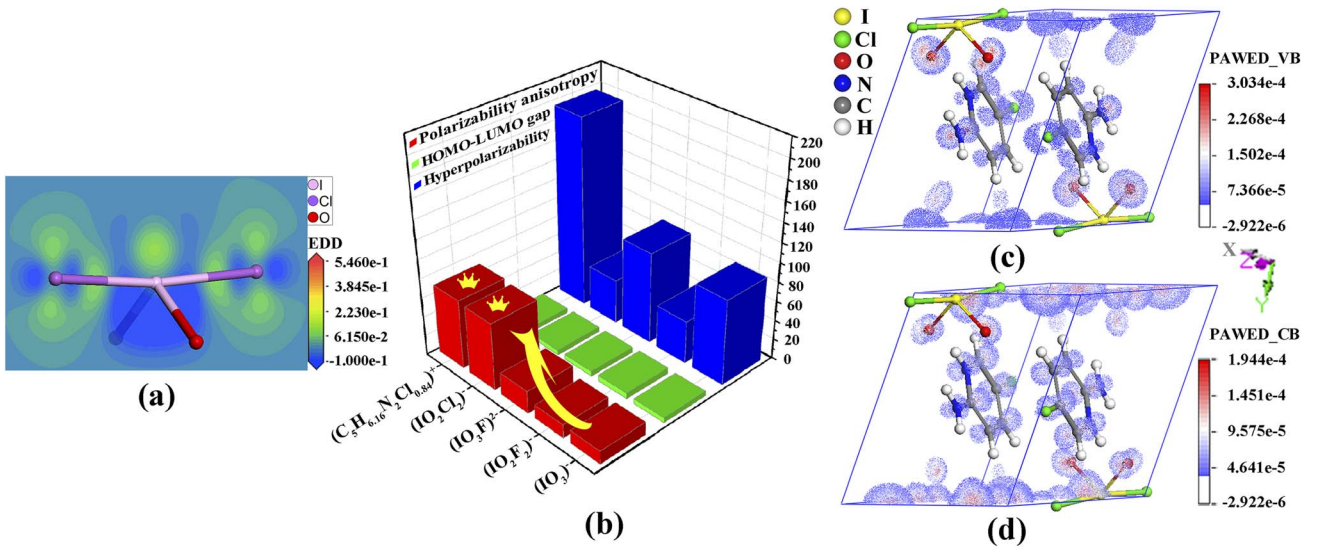

Fig. 3 Electron density difference map of the $(IO_2Cl_2)^-$ group (a), some properties of the related groups (b), and the polarizability anisotropy-weighted electron density in the VB (c) and CB (d) for $(C_5H_{6.16}N_2Cl_{0.84})(IO_2Cl_2)$.

$(C_5H_{6.16}N_2Cl_{0.84})^+$ play a pivotal role in enhancing birefringence. In the CB, the birefringence chiefly originates from the unoccupied I-5p along with Cl-3p and O-2p states of $(IO_2Cl_2)^-$, and the C-2p and N-2p states in $(C_5H_{6.16}N_2Cl_{0.84})^+$. Thus, the exceptional birefringence is synergistically determined by $(IO_2Cl_2)^-$ and $(C_5H_{6.16}N_2Cl_{0.84})^+$ groups with the precise contribution values of 62.9% and 37.1%, respectively. This also demonstrates that the $(IO_2Cl_2)^-$ group is a highly effective birefringent-active group.

Conclusions

In summary, we have isolated a new birefringent crystal $(C_5H_{6.16}N_2Cl_{0.84})(IO_2Cl_2)$ composed of unprecedented $(IO_2Cl_2)^-$ anions and π-conjugated $(C_5H_{6.16}N_2Cl_{0.84})^+$ cations. It displays very large birefringence of 0.67 at 546 nm, and thus it is a new candidate for visible birefringent materials. This work initiates research on the chloroiodate(v) system and affords a new route for the design of excellent birefringent materials.

Author contributions

Qian–Qian Chen: conceptualization, data curation, methodology, visualization, writing – original draft; Chun-Li Hu: formal analysis; Ming-Zhi Zhang: data curation; Jiang-Gao Mao: conceptualization, writing – review & editing, supervision.

Conflicts of interest

There are no conflicts to declare.

Acknowledgements

This work was financially supported by the National Natural Science Foundation of China (no. 22375201, 22031009, 21921001, and 21975256).

Notes and references

1 L. H. Nicholls, F. J. Rodríguez-Fortuño, M. E. Nasir, R. M. Córdova-Castro, N. Olivier, G. A. Wurtz and A. V. Zayats, Ultrafast Synthesis and Switching of Light Polarization in Nonlinear Anisotropic Metamaterials, *Nat. Photonics*, 2017, **11**, 628–633.

2 X. M. Chen, W. G. Lu, J. L. Tang, Y. Y. Zhang, Y. T. Wang, G. D. Scholes and H. Z. Zhong, Solution-Processed Inorganic Perovskite Crystals as Achromatic Quarter-Wave Plates, *Nat. Photonics*, 2021, **15**, 813–816.

3 M. Mutailipu, K. R. Poeppelmeier and S. L. Pan, Borates: A Rich Source for Optical Materials, *Chem. Rev.*, 2021, **121**, 1130–1202.

4 Z. Y. Bai, J. Lee, H. Kim, C. L. Hu and K. M. Ok, Unveiling the Superior Optical Properties of Novel Melamine-Based Nonlinear Optical Material with Strong Second-Harmonic Generation and Giant Optical Anisotropy, *Small*, 2023, **19**, 2301756–2301761.

5 S. Y. Niu, G. Joe, H. Zhao, Y. C. Zhou, T. Orvis, H. X. Huyan, J. Salman, K. Mahalingam, B. Urwin, J. B. Wu, Y. Liu, T. E. Tiwald, S. B. Cronin, B. M. Howe, M. Mecklenburg, R. Haiges, D. J. Singh, H. Wang, M. A. Kats and J. Ravichandran, Giant Optical Anisotropy in a Quasi-One-Dimensional Crystal, *Nat. Photonics*, 2018, **12**, 392–396.

6 S. J. Han, A. Tudi, W. B. Zhang, X. L. Hou, Z. H. Yang and S. L. Pan, Recent Development of Sn^{II}, Sb^{III}-based Birefringent Material: Crystal Chemistry and Investigation of Birefringence, *Angew. Chem., Int. Ed.*, 2023, **62**, e202302025.

7 G. Ghosh, Dispersion-Equation Coefficients for the Refractive Index and Birefringence of Calcite and Quartz Crystals, *Opt. Commun.*, 1999, **163**, 95–102.

8 H. T. Luo, T. Tkaczyk, E. L. Dereniak, K. Oka and R. Sampson, High Birefringence of the Yttrium Vanadate Crystal in the Middle Wavelength Infrared, *Opt. Lett.*, 2006, **31**, 616–618.

9 D. V. Grudinin, G. A. Ermolaev, D. G. Baranov, A. N. Toksumakov, K. V. Voronin, A. S. Slavich, A. A. Vyshnevyy, A. B. Mazitov, I. A. Kruglov, D. A. Ghazaryan, A. V. Arsenin, K. S. Novoselov and V. S. Volkov, Hexagonal Boron Nitride Nanophotonics: A Record-Breaking Material for the Ultraviolet and Visible Spectral Ranges, *Mater. Horiz.*, 2023, **10**, 2427–2435.

10 Y. Q. Li, X. Zhang, J. Y. Zheng, Y. Zhou, W. Q. Huang, Y. P. Song, H. Wang, X. Y. Song, J. H. Luo and S. G. Zhao, A Hydrogen Bonded Supramolecular Framework Birefringent Crystal, *Angew. Chem., Int. Ed.*, 2023, **62**, e202304498.

11 J. Y. Guo, A. Tudi, S. J. Han, Z. H. Yang and S. L. Pan, Sn_2PO_4I: An Excellent Birefringent Material with Giant Optical Anisotropy in Non π-Conjugated Phosphate, *Angew. Chem., Int. Ed.*, 2021, **60**, 24901–24904.

12 J. Y. Guo, J. B. Huang, A. Tudi, X. L. Hou, S. J. Han, Z. H. Yang and S. L. Pan, Birefringence Regulation by Clarifying the Relationship Between Stereochemically Active Lone Pairs and Optical Anisotropy in Tin-based Ternary Halides, *Angew. Chem., Int. Ed.*, 2023, **62**, e202304238.

13 J. Y. Guo, A. Tudi, S. J. Ha, Z. H. Yang and S. L. Pan, α-SnF_2: A UV Birefringent Material with Large Birefringence and Easy Crystal Growth, *Angew. Chem., Int. Ed.*, 2021, **60**, 3540–3544.

14 J. Y. Guo, A. Tudi, S. J. Han, Z. H. Yang and S. L. Pan, $Sn_2B_5O_9Cl$: A Material with Large Birefringence Enhancement Activated Prepared via Alkaline-Earth-Metal Substitution by Tin, *Angew. Chem., Int. Ed.*, 2019, **58**, 17675–17678.

15 C. Wu, X. X. Jiang, Z. J. Wang, L. Lin, Z. S. Lin, Z. P. Huang, X. F. Long, M. G. Humphrey and C. Zhang, Giant Optical Anisotropy in the UV-Transparent 2D Nonlinear Optical Material $Sc(IO_3)_2(NO_3)$, *Angew. Chem., Int. Ed.*, 2021, **60**, 3464–3468.

16 Y. Huang, Z. Fang, B. P. Yang, X. Y. Zhang and J. G. Mao, A New Birefringent Material, $HfF_2(IO_3)_2$, with a Large Birefringence and Improved Overall Performances Achieved by the Integration of Functional Groups, *Scr. Mater.*, 2023, **223**, 115082–115086.

17 T. H. Wu, X. X. Jiang, Y. R. Zhang, Z. J. Wang, H. Y. Sha, C. Wu, Z. S. Lin, Z. P. Huang, X. F. Long, M. G. Humphrey and C. Zhang, From $CeF_2(SO_4)\cdot H_2O$ to $Ce(IO_3)_2(SO_4)$: Defluorinated Homovalent Substitution for Strong Second-Harmonic-Generation Effect and Sufficient Birefringence, *Chem. Mater.*, 2021, **33**, 9317–9325.

18 F. F. Mao, C. L. Hu, X. Xu, D. Yan, B. P. Yang and J. G. Mao, $Bi(IO_3)F_2$: The First Metal Iodate Fluoride with a Very Strong Second Harmonic Generation Effect, *Angew. Chem., Int. Ed.*, 2017, **56**, 2151–2155.

19 Q. Wu, H. M. Liu, F. C. Jiang, L. Kang, L. Yang, Z. S. Lin, Z. G. Hu, X. G. Chen, X. G. Meng and J. G. Qin, $RbIO_3$ and $RbIO_2F_2$: Two Promising Nonlinear Optical Materials in Mid-IR Region and Influence of Partially Replacing Oxygen with Fluorine for Improving Laser Damage Threshold, *Chem. Mater.*, 2016, **28**, 1413–1418.

20 M. Zhang, C. Hu, T. Abudouwufu, Z. H. Yang and S. L. Pan, Functional Materials Design via Structural Regulation Originated from Ions Introduction: A Study Case in Cesium Iodate System, *Chem. Mater.*, 2018, **30**, 1136–1145.

21 M. Q. Gai, T. H. Tong, Y. Wang, Z. H. Yang and S. L. Pan, New Alkaline-Earth Metal Fluoroiodates Exhibiting Large Birefringence and Short Ultraviolet Cutoff Edge with Highly Polarizable $(IO_3F)^{2-}$ Units, *Chem. Mater.*, 2020, **32**, 5723–5728.

22 Y. L. Hu, X. X. Jiang, T. H. Wu, Y. Y. Xue, C. Wu, Z. P. Huang, Z. S. Lin, J. Xu, M. G. Humphrey and C. Zhang, Wide Bandgaps and Strong SHG Responses of Hetero-Oxyfluorides by Dual-Fluorination-Directed Bandgap Engineering, *Chem. Sci.*, 2022, **13**, 10260–10266.

23 Z. H. Chen, Z. Z. Zhang, R. L. Wu, X. Y. Dong, Y. J. Shi and Q. Jing, Theoretical Study on $Pb_2VO_2F_5$: Large Birefringence Derived from Optical Anisotropies of VO_2F_4 Groups, *J. Mater. Sci.*, 2018, **53**, 3483–3492.

24 J. J. Zhou, H. P. Wu, H. W. Yu, S. T. Jiang, Z. G. Hu, J. Y. Wang, Y. C. Wu and P. S. Halasyamani, $BaF_2TeF_2(OH)_2$: A UV Nonlinear Optical Fluorotellurite Material Designed by Band-Gap Engineering, *J. Am. Chem. Soc.*, 2020, **142**, 4616–4620.

25 R. Fu, R. J. Nielsen, N. S. Liebov, W. A. Goddard III, T. B. Gunnoe and J. T. Groves, DFT Mechanistic Study of Methane Mono-Esterification by Hypervalent Iodine Alkane Oxidation Process, *J. Phys. Chem. C*, 2019, **123**, 15674–15684.

26 J. J. Wu, Y. Guo, J. L. Qi, W. D. Yao, S. X. Yu, W. L. Liu and S. P. Guo, Multi-Stimuli Responsive Luminescence and Domino Phase Transition of Hybrid Copper Halides with Nonlinear Optical Switching Behavior, *Angew. Chem., Int. Ed.*, 2023, **62**, e202301937.

27 M. Kalmutzki, M. Strçbele, F. Wackenhut, A. J. Meixner and H. J. Meyer, Synthesis, Structure, and Frequency-Doubling Effect of Calcium Cyanurate, *Angew. Chem., Int. Ed.*, 2014, **53**, 14260–14263.

28 Q. Q. Chen, C. L. Hu, J. Chen, Y. L. Li, B. X. Li and J. G. Mao, $[o\text{-}C_5H_4NHOH]_2[I_7O_{18}(OH)]\cdot 3H_2O$: An Organic-Inorganic Hybrid SHG Material Featuring an $[I_7O_{18}(OH)]_\infty^{2-}$ Branched Polyiodate Chain, *Angew. Chem., Int. Ed.*, 2021, **60**, 17426–17429.

29 J. Lu, X. Liu, M. Zhao, X. B. Deng, K. X. Shi, Q. R. Wu, L. Chen and L. M. Wu, Discovery of NLO Semiorganic $(C_5H_6ON)^+(H_2PO_4)^-$: Dipole Moment Modulation and Superior Synergy in Solar-Blind UV Region, *J. Am. Chem. Soc.*, 2021, **143**, 3647–3654.

30 D. H. Lin, M. Luo, C. S. Lin, F. Xu and N. Ye, $KLi(HC_3N_3O_3)\cdot 2H_2O$: Solvent-drop Grinding Method toward the Hydro-isocyanurate Nonlinear Optical Crystal, *J. Am. Chem. Soc.*, 2019, **141**, 3390–3394.

31 X. H. Meng, X. Y. Zhang, Q. X. Liu, Z. Y. Zhou, X. X. Jiang, Y. G. Wang, Z. S. Lin and M. J. Xia, Perfectly Encoding π-Conjugated Anions in the $RE_5(C_3N_3O_3)(OH)_{12}$ (RE = Y, Yb, Lu) Family with Strong Second Harmonic Generation Response and Balanced Birefringence, *Angew. Chem., Int. Ed.*, 2022, **62**, e202214848.

32 Y. Q. Li, X. Zhang, Y. Zhou, W. Q. Huang, Y. P. Song, H. Wang, M. J. Li, M. C. Hong, J. H. Luo and S. G. Zhao, An Optically Anisotropic Crystal with Large Birefringence Arising from Cooperative π Orbitals, *Angew. Chem., Int. Ed.*, 2022, **61**, e202208811.

33 G. Peng, C. S. Lin, H. X. Fan, K. C. Chen, B. X. Li, G. Zhang and N. Ye, $Be_2(BO_3)(IO_3)$: The First Anion-mixed Van der Waals Member in the $KBe_2BO_3F_2$ Family with a Very Strong Second Harmonic Generation Response, *Angew. Chem., Int. Ed.*, 2021, **60**, 17415–17418.

34 A. Azaid, M. Alaqarbeh, T. Abram, M. Raftani, R. Kacimi, Y. Khaddam, A. Sbai, T. Lakhlifi and M. Bouachrine, D-π-A Push-Pull Chromophores Based on N,N-Diethylaniline as a Donor for NLO Applications: Effects of Structural Modification of π-Linkers, *J. Mol. Struct.*, 2024, **1295**, 136602–136612.

35 H. Robert and S. Urs, *US Pat.*, US5274100A, (Ciba-Geigy Corporation), 1993.

36 D. Hausmann, A. Eich and C. Feldmann, The Mixed Valence Iodine Chlorides $[PCl_4]_2[ICl_2][ICl_4]$ and $[BnMe_3N]_2[I_2Cl_3][ICl_4]$, *J. Mol. Struct.*, 2018, **1166**, 159–163.

37 I. D. Brown and D. Altermatt, Comprehensive Derivation of Bond-Valence Parameters for Ion Pairs Involving Oxygen, *Acta Crystallogr., Sect. B: Struct. Sci., Cryst. Eng. Mater.*, 2015, **71**, 562–578.

38 K. Nakamoto, *Theory and Applications in Inorganic Chemistry*, Wiley, Hoboken, NJ, 1997.

39 Y. J. Jia, Y. G. Chen, T. Wang, Y. Guo, X. F. Guan and X. M. Zhang, High Coordinate Metal Iodate Chlorides with Diverse Structural Motifs and Tunable Birefringence, *Cryst. Growth Des.*, 2020, **20**, 5473–5483.

40 W. Q. Huang, X. Zhang, Y. Q. Li, Y. Zhou, X. Chen, X. Q. Li, F. F. Wu, M. C. Hong, J. H. Luo and S. G. Zhao, A Hybrid Halide Perovskite Birefringent Crystal, *Angew. Chem., Int. Ed.*, 2022, **61**, e202202746.

41 Y. J. Cui, Y. F. Yue, G. D. Qian and B. L. Chen, Luminescent Functional Metal-Organic Frameworks, *Chem. Rev.*, 2012, **112**, 1126–1162.

42 J. Lu, Y. K. Lian, L. Xiong, Q. R. Wu, M. Zhao, K. X. Shi, L. Chen and L. M. Wu, How To Maximize Birefringence and Nonlinearity of π-Conjugated Cyanurates, *J. Am. Chem. Soc.*, 2019, **141**, 16151–16159.

43 Y. C. Liu, X. M. Liu, S. Liu, Q. R. Ding, Y. Q. Li, L. N. Li, S. G. Zhao, Z. S. Lin, J. H. Luo and M. C. Hong, An Unprecedented Antimony(III) Borate with Strong Linear and Nonlinear Optical Responses, *Angew. Chem., Int. Ed.*, 2020, **59**, 7793–7796.

44 B. C. Wu, D. Y. Tang, N. Ye and C. T. Chen, Linear and Nonlinear Optical Properties of the $KBe_2BO_3F_2$ (KBBF) Crystal, *Opt. Mater.*, 1996, **5**, 105–109.

45 Z. P. Zhang, X. Liu, X. M. Liu, Z. W. Lu, X. Sui, B. Y. Zhen, Z. S. Lin, L. Chen and L. M. Wu, Driving Nonlinear Optical Activity with Dipolar 2-Aminopyrimidinium Cations in $(C_4H_6N_3)^+(H_2PO_3)^-$, *Chem. Mater.*, 2022, **34**, 1976–1984.

46 Y. L. Deng, L. Huang, X. H. Dong, L. Wang, K. M. Ok, H. M. Zeng, Z. E. Lin and G. H. Zou, $K_2Sb(P_2O_7)F$: Cairo Pentagonal Layer with Bifunctional Genes Reveal Optical Performance, *Angew. Chem., Int. Ed.*, 2020, **59**, 21151–21156.

47 M. J. Dodge, Refractive Properties of Magnesium Fluoride, *Appl. Opt.*, 1984, **23**, 1980–1985.

48 X. H. Dong, L. Huang, H. M. Zeng, Z. E. Lin, K. M. Ok and G. H. Zou, High-Performance Sulfate Optical Materials Exhibiting Giant Second Harmonic Generation and Large Birefringence, *Angew. Chem., Int. Ed.*, 2022, **61**, e202116790.

49 C. Wu, T. H. Wu, X. X. Jiang, Z. J. Wang, H. Y. Sha, L. Lin, Z. S. Lin, Z. P. Huang, X. F. Long, M. G. Humphrey and C. Zhang, Large Second-Harmonic Response and Giant Birefringence of $CeF_2(SO_4)$ Induced by Highly Polarizable Polyhedra, *J. Am. Chem. Soc.*, 2021, **143**, 4138–4142.

50 C. C. Jin, F. M. Li, B. L. Cheng, H. T. Qiu, Z. H. Yang, S. L. Pan and M. Mutailipu, Double-Modification Oriented Design of a Deep-UV Birefringent Crystal Functionalized by $[B_{12}O_{16}F_4(OH)_4]$ Clusters, *Angew. Chem., Int. Ed.*, 2022, **61**, e20220398.

51 C. C. Jin, F. M. Li, Z. H. Yang, S. L. Pan and M. Mutailipu, $[C_3N_6H_7]_2[B_3O_3F_4(OH)]$: A New Hybrid Birefringent Crystal with Strong Optical Anisotropy Induced by Mixed Functional Units, *J. Mater. Chem. C*, 2022, **10**, 6590–6595.

52 J. Lu, J. N. Yue, L. Xiong, W. K. Zhang, L. Chen and L. M. Wu, Uniform Alignment of Non-π-Conjugated Species Enhances Deep Ultraviolet Optical Nonlinearity, *J. Am. Chem. Soc.*, 2019, **141**, 8093–8097.